Development 137, 3303-3313 (2010) doi:10.1242/dev.047332

Recognition of pre- and postsynaptic neurons via nephrin/NEPH1 homologs is a basis for the formation of the *Drosophila* retinotopic map

Atsushi Sugie[1,2], Daiki Umetsu[1,2,*], Tetsuo Yasugi[1,2], Karl-Friedrich Fischbach[3] and Tetsuya Tabata[1,†]

SUMMARY

Topographic maps, which maintain the spatial order of neurons in the order of their axonal connections, are found in many parts of the nervous system. Here, we focus on the communication between retinal axons and their postsynaptic partners, lamina neurons, in the first ganglion of the *Drosophila* visual system, as a model for the formation of topographic maps. Post-mitotic lamina precursor cells differentiate upon receiving Hedgehog signals delivered through newly arriving retinal axons and, before maturing to extend neurites, extend short processes toward retinal axons to create the lamina column. The lamina column provides the cellular basis for establishing stereotypic synapses between retinal axons and lamina neurons. In this study, we identified two cell-adhesion molecules: Hibris, which is expressed in post-mitotic lamina precursor cells; and Roughest, which is expressed on retinal axons. Both proteins belong to the nephrin/NEPH1 family. We provide evidence that recognition between post-mitotic lamina precursor cells and retinal axons is mediated by interactions between Hibris and Roughest. These findings revealed mechanisms by which axons of presynaptic neurons deliver signals to induce the development of postsynaptic partners at the target area. Postsynaptic partners then recognize the presynaptic axons to make ensembles, thus establishing a topographic map along the anterior/posterior axis.

KEY WORDS: *Drosophila*, Hibris, Roughest, Retinotopic map

INTRODUCTION

Topographic maps, which maintain the spatial organization of neurons in the order of their axonal connections, are found throughout the nervous system (Udin and Fawcett, 1988). A notable model of topographic map formation is found in the visual system, in which a relay of visual information is arranged in a spatially ordered manner from the retina to the visual center in the brain. This topographic map is termed a retinotopic map. The *Drosophila* visual system has also provided insights into retinotopic mapping and has been a useful model for studying the mechanisms underlying the communication between pre- and postsynaptic neurons (Ting and Lee, 2007). During the development of the *Drosophila* visual center, presynaptic photoreceptors extend retinal (R) axons to the first optic ganglion, the lamina layer. Postsynaptic lamina precursor cells (LPC) start to differentiate in response to Hedgehog (Hh), which is delivered through newly arriving R axons and become post-mitotic lamina precursor cells (pLPCs) expressing Dachshund (Dac). pLPCs then form stereotyped ensembles known as lamina columns in a posterior-to-anterior direction in a stepwise manner (Huang and Kunes, 1996; Meinertzhagen and Hanson, 1993) and a subset of pLPCs becomes specified as the lamina neurons (LNs) L1-L5 (Huang and Kunes, 1998; Huang et al., 1998). Formation of these columns is fundamental to the subsequent establishment of intricate synaptic connections (Clandinin and Zipursky, 2002; Meinertzhagen and Hanson, 1993). During the differentiation of pLPCs, Hh induces Single-minded (Sim) expression in pLPCs. Sim, a bHLH transcription factor, is required for pLPCs to establish an association with the corresponding R axons (Umetsu et al., 2006). This process is unique in that presynaptic neurons regulate the development of postsynaptic partners in the target area, and the presynaptic and postsynaptic neurons make stereotypic ensembles in an early stage of development before synapse formation. This step-by-step mechanism seems to be an efficient way to make a precise topographic map along the anterior/posterior axis. However, the molecular basis underlying cell-cell interactions between R axons and pLPCs is largely unknown.

Multiple classes of cell-surface molecules are involved in cell-cell recognition in the *Drosophila* visual system (Ting and Lee, 2007). We identified a cell surface molecule called Hibris (Hbs), which is expressed in pLPCs and is required for lamina column assembly. Hbs belongs to the nephrin protein family. Nephrin and NEPH1 proteins are members of the immunoglobulin superfamily, which includes transmembrane proteins that mediate Ca^{2+}-independent cell-cell adhesion (Barclay and Robertson, 2003; Hynes and Lander, 1992). In *Drosophila*, two nephrin homologs, Hbs and Sticks-and-stones (Sns), and two NEPH1 homologs, irreC/Roughest (Rst) and Kin of irre (Kirre, also called Dumbfounded), have been identified (Artero et al., 2001; Bour et al., 2000; Dworak et al., 2001; Ramos et al., 1993; Strunkelnberg et al., 2001). These proteins are known as the irre cell recognition module (IRM) proteins (Fischbach et al., 2009) and are suggested to function through direct homophilic or heterophilic binding with other nephrin/NEPH1 homologs during processes such as the formation of the nephrocytes (Zhuang et al., 2009), myoblast fusion (Galletta et al., 2004; Shelton et al., 2009), cell sorting in

[1]Institute of Molecular and Cellular Biosciences, The University of Tokyo, Yayoi 1-1-1, Bunkyo-ku, Tokyo 113-0032, Japan. [2]Graduate program in Biophysics and Biochemistry, Graduate School of Science, The University of Tokyo, Hongo 7-3-1, Bunkyo-ku, Tokyo 113-0033, Japan. [3]Department of Neurobiology, Faculty of Biology, Albert-Ludwigs-University Freiburg, Germany.

*Present address: Max-Planck Institute of Molecular Cell Biology and Genetics, Pfotenhauerstrasse 108, 01307 Dresden, Germany
†Author for correspondence (ttabata@iam.u-tokyo.ac.jp)

Accepted 21 July 2010

eye morphogenesis (Bao and Cagan, 2005) and axonal pathfinding in the visual system (Fischbach et al., 2009; Ramos et al., 1993; Schneider et al., 1995). Bao and Cagan identified Hbs in primary pigment cells and showed that its preferential adhesion to Rst is required for cell sorting to occur (Bao and Cagan, 2005). Proteins of the nephrin and NEPH subfamilies are also expressed in neighboring cell types in the nervous system of vertebrates (Beltcheva et al., 2003; Gerke et al., 2006; Morikawa et al., 2007; Tamura et al., 2005). The homophilic interaction of Kirrel3, a member of the NEPH subfamily, has been shown to be involved in the axonal fasciculation of olfactory sensory neurons (Serizawa et al., 2006).

We examined the roles of Hbs and its partner Rst during the first step of lamina column assembly. Hbs-Rst interaction is required for lamina column assembly at this early stage, and this provides the basis for further steps in lamina development, eventually leading to topographically correct synapse formation.

MATERIALS AND METHODS

Genetics

yw flies were used as wild-type controls. The following mutant strains were used in this study: sim^{2} and sim^{ry75} (Pielage et al., 2002), hbs^{459} (Artero et al., 2001), *Df(2R)14* (Denholm et al., 2003), $irreC^{1R34}$ and rst^{CT} (Schneider et al., 1995), *Df(1)rst-vt* (Ruiz-Gomez et al., 2000) and $Df(1)duf^{ps\text{-}1}$ (Weavers et al., 2009). The following transgenic strains were used in this study: *UAS-GFPnls* and *UAS-mCD8GFP* (Lee and Luo, 1999), *UAS-sim* (Chang et al., 2003), *UAS-hbs FL* (Dworak et al., 2001), *UAS-hbs-ECD* and *UAS-hbs-ICD* (Artero et al., 2001), *UAS-hbs-HA* (Shelton et al., 2009), *UAS-rst FL*, known as *UAS-HB3* (Schneider et al., 1995), *UAS-rst-DD1* (Vishnu et al., 2006), *NP6099-Gal4* (Hayashi et al., 2002; Yoshida et al., 2005), *GMR-Gal4* (Hay et al., 1997), *hs-flp122; AyGal4* (Ito et al., 1997) and $ey^{3.5}$*-FLP* (Bazigou et al., 2007). *UAS-dsRNA* lines (*hbs*; 40898, *sns*; 877, *rst*; 27225, *kirre*; 3111) and *UAS-dicer2* lines (60008, 60009) were obtained from the VDRC stock center.

Labeling a subset of post-mitotic lamina precursor cells with GFP

hsflp122; *AyGal4, UAS-GFP/UAS-CD8GFP* was used for labeling a random subset of pLPCs. For labeling a subset of pLPCs in sim^{2}/sim^{ry75} mutants, males with the genotype of *hsflp122*; *AyGal4, UAS-GFP*; sim^{ry75} were mated with *UAS-CD8GFP*; sim^{2} females. The progeny at 72-96 hours after egg laying (AEL) were heat shocked (37°C for 40 minutes). Dissections were carried out at the late third instar larval stage.

Quantification of the number of pLPCs extending processes to R axons

To assess the interaction between pLPCs and R axons, the number of pLPCs extending processes to R axons in control flies and *sim* mutants was counted in confocal images of the optic lobe. Each process was defined as an extended protrusion of more than 2 μm. The interaction between pLPCs and R axons was defined by contact between the tip of the processes and R axons.

Clonal analysis

sim^{2} clones were induced using *FRT82B,* sim^{2} and *hsflp;; FRT82B, ubi-GFP,* $M(3)^{w124}$ (Ferrus, 1975). After these strains were mated, the progeny at 24-48 hours AEL were heat shocked (37°C for 1 hour). Dissections were carried out at the late third instar larval stage.

Histology

Immunohistochemistry was performed as previously described (Huang and Kunes, 1996; Takei et al., 2004). The following antibodies were used in this study: mouse anti-Dac (mAbdac2-3, 1:1000, DSHB), mouse anti-Dlg (4F3, 1:20, DSHB), mouse anti-Chaoptin (mAb24B10, 1:10, DSHB), mouse anti-HA (1:500, Covance), mouse anti-Rst [MAb24A5.1, 1:50, (Schneider et al., 1995)], rat anti-Elav (7E8A10, 1:50, DSHB), rat anti-Shg (DCAD2, 1:20, DSHB), rabbit anti-Kirre [A126i, 1:400, (Kreiskother et al., 2006)], rabbit anti-Sns [1:400, (Kesper et al., 2007)], rabbit anti-GFP (1:500, Medical and Biological Laboratories CO., LTD.), goat Cy3 anti-HRP and goat FITC anti-HRP (1:800, Accurate Chemical and Scientific). The anti-Hbs antibody (1:500) was generated by Operon Biotechnologies (Tokyo) against the mixed peptides NH2- C+RPLDNSTYKTTSSSD -COOH, NH2- C+LPNPKRHSQRNSATG -COOH and NH2- C+FNMSDKYMSYPPVTY -COOH in rats. Secondary antibodies (Jackson) were used at the following dilutions: anti-mouse Cy3, 1:200; anti-mouse Cy5, 1:200; anti-rat Cy3, 1:200; anti-rat Cy5, 1:200; anti-rabbit Cy5, 1:200; anti-rabbit Alexa 660, 1:200; and anti-rabbit FITC, 1:200 (Molecular Probes). Specimens were mounted with Vectashield mounting medium (Vector) and viewed on a Zeiss LSM710 confocal microscope.

Quantification of lamina column assembly

The ratio of the number of Dac-positive cells of the assembling domain to that of the entire lamina domain was calculated to compare lamina column assembly in control flies, *hbs* mutants and *rst* mutants. To optically dissect the assembling domain from the pre-assembling domain of the lamina in the late 3rd instar larval stage, projections of the confocal images were subjected to Amira (Visage Imaging GmbH) and ImageJ software (National Institutes of Health, Bethesda, MD, USA). The datasets were then subjected to a developmental version of Eve software (Kamikouchi et al., 2006) (T. Shimada, K. Kato, H. Otsuna and K. Ito, unpublished) to count the cells labeled with the anti-Dac antibody. There was no statistical difference between the cell numbers counted with Eve software and those counted manually.

Microarray analysis

The lamina was isolated from late third larval brains to compare the comprehensive gene expression profiles of *yw/NP6099;UAS-CD8GFP/+;*sim^{2}/sim^{ry75} (n=3; 412, 496 and 500 laminas) with those of *yw/NP6099;UAS-CD8GFP/+* (n=3; 423, 452 and 448 laminas). Total RNA was prepared from dissected lamina cells by Bio Matrix Research (Chiba). Biotinylated cRNA was then prepared and hybridized to an Affymetrix *Drosophila* Genome 2.0 array by Bio Matrix Research (Chiba). To identify candidate genes whose expression levels were altered in the *sim* mutant, the data were analyzed using GeneSpring GX software (Agilent).

RESULTS

pLPCs extend processes toward R axons in the first step of lamina column assembly

During development of the *Drosophila* visual center, presynaptic photoreceptors extend their axons to the first optic ganglion lamina layer (Fig. 1A-F). Retinal (R) axons establish stereotypic connections with developing lamina neurons (LNs) and form ensembles known as lamina columns in a posterior to anterior order (Fig. 1E,F; Meinertzhagen and Hanson, 1993). Here, we refer to the region that is not innervated by R axons as the pre-assembling domain and the region that is innervated as the assembling domain (Fig. 1B,C,E,F, arrowed lines). In the pre-assembling domain, post-mitotic lamina precursor cells (pLPCs) express the differentiation marker Dachshund (Dac). We also detected Dac in the inner proliferation center (Fig. 1C, white arrowhead). Most IPC cells give rise to the cell body layer of the lobula plate. In addition to Dac expression, LNs begin expressing the neuronal marker for embryonic lethal abnormal vision (Elav) in the assembling domain as they differentiate into mature LNs in later developmental stages (Huang and Kunes, 1996; Huang et al., 1998; Umetsu et al., 2006). Differentiation of lamina precursor cells (LPCs) is induced by Hedgehog (Hh) secreted from newly arriving R axons (Huang and Kunes, 1996). At the same time, Hh induces the expression of the transcription factor *single-minded* (*sim*) gene in pLPCs. pLPCs in the pre-assembling domain were shown to require Sim for at least the first step of lamina column assembly (Umetsu et al., 2006). Because the cellular mechanisms underlying this process have not been elucidated, we looked closely at the cell shape of the pLPCs that were about to integrate into the

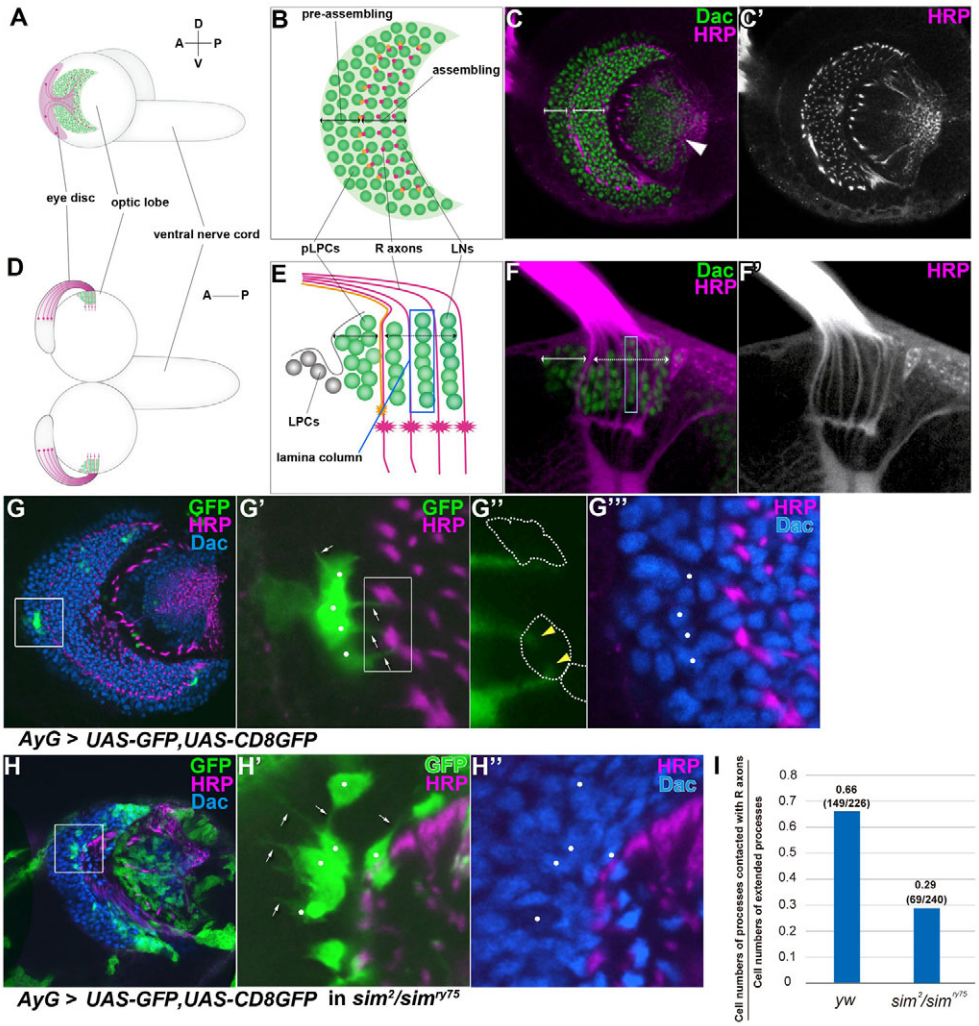

Fig. 1. The onset of lamina column assembly depends on the activity of Single-minded. (**A**,**D**) Schematic drawings of the *Drosophila* central nervous system in the late third instar larval stage from lateral (A) and horizontal (D) perspectives. Unless otherwise noted, all images are of the late third instar larval stage. A, anterior; P, posterior; D, dorsal; V, ventral. (**B**,**E**) Schematic drawings of lamina from lateral (B) and horizontal (E) perspectives. During the development of the lamina, photoreceptor cells in the eye disc extend their R axons (magenta) to the first optic ganglion: the lamina layer (green). Soon after LPCs start to differentiate into pLPCs, they form close associations with newly arriving R axons and make stereotyped ensembles, known as lamina columns (blue rectangle), in a posterior-to-anterior direction and step-wise manner. The lamina is divided into two domains: the pre-assembling domain, which is not innervated by R axons, and the assembling domain, which is innervated (black arrowed lines). pLPCs primarily exist in the pre-assembling domain. Subsets of LNs exist in the assembling domain. (**C**,**F**) Confocal images of the optic lobe immunostained for Dac (pLPCs and LNs, green) and HRP (R axons, magenta) from lateral (C) and horizontal (F) views. The inner proliferation center are shown (white arrowhead). Arrows and rectangles as in B,E. (C′,F′) HRP in C and F. (**G-H″**) Subsets of pLPCs were clonally labeled by GFP (green) in *yw* (G) or sim^{2}/sim^{ry75} (H). (G′,G‴,H′,H″) Magnified images of the area outlined in G and H. (G″) Higher magnification of the area outlined in G′. The areas stained by anti-HRP are outlined. The tips of the pLPCs that contact R axons are indicated by yellow arrowheads. pLPCs and LNs in the optic lobe are visualized by anti-Dac (blue). pLPCs (G′,G‴, white circles) extend their processes to R axons in the control animal samples (G′, arrows). However, pLPCs in *sim* mutants (H′,H″, white circles) occasionally failed to direct to R axons (H′, arrows). (**I**) Quantification of the ratio of the number of cells extending protrusions to R axons in *yw* (0.66: 149/226) and sim^{2}/sim^{ry75} mutants (0.29: 69/240). The protrusions were defined as extended processes greater than 2 μm in length. The extended protrusions to R axons were defined by contact between the tip of the pLPCs and R axons.

lamina column. In order to visualize cell shape, we randomly marked pLPCs with GFP. The pLPCs often extended cellular processes (Fig. 1G′, arrows) and contacted newly arriving R axons (Fig. 1G″, yellow arrowheads). In a heteroallelic combination of the *sim* mutants, pLPCs still formed processes, but smaller number of cells contacted R axons compared with control flies (Fig. 1H′, arrows). We calculated the ratio of pLPCs with processes that were in contact with R axons to all pLPCs with processes and found that this ratio was significantly smaller in *sim* mutants (Fig. 1I, 0.29: 69/240 pLPCs) than in the control (Fig. 1I, 0.66: 149/226 pLPCs). We reasoned that Sim is required for pLPCs to establish and/or maintain a direct interaction with R axons, probably through regulating the expression of cell surface molecules that are required for R axon association.

The cell-adhesion molecule Hibris is expressed in pLPCs under the control of Sim

To identify molecules that play roles in intercellular communication at the cell surface of pLPCs, we searched for the downstream effectors of Sim using microarray analysis (see materials and

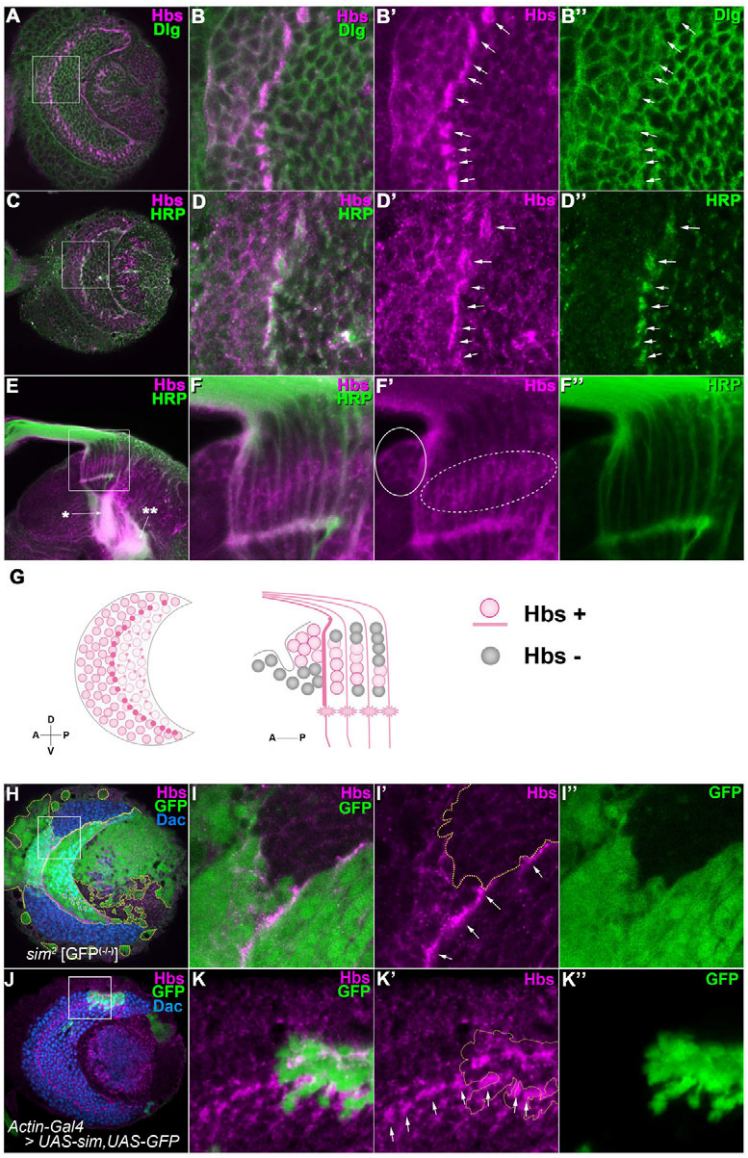

Fig. 2. The expression of Hbs is dependent on Sim. (**A-F″**) Confocal images of the *Drosophila* optic lobe immunostained for Hbs protein (magenta) in *yw*. Hbs is localized on the membrane of pLPCs (A-B″). Plasma membranes are visualized by anti-Dlg (A-B″, green). Hbs is strongly expressed in the most anterior R axons (D-D″, arrows) and seems to accumulate at the contact surface between pLPCs and R axons (B-B″,D-D″, arrows). R axons are visualized by anti-HRP (D-F″, green). Staining of Hbs is also seen in the medulla neuropil (E, asterisk) and lobula neuropil (E, double asterisk). Hbs expression is high in the region close to the optic stalk in the pre-assembling domain (E-F″, white outline) and is restricted in the assembling domain (E-F″, broken white outline). Lateral (A,C) and horizontal (E) sections of the optic lobe are shown. (B-B″,D-D″,F-F″) Magnified images of the areas outlined in A,C,E. (**G**) Schematic drawings of Hbs staining. The stained region (+) is shown in magenta. (**H-I″**) Confocal image of the optic lobe immunostained for Hbs in sim^2 clones, which are indicated by the absence of GFP (green). pLPCs and LNs are visualized using anti-Dac (blue). (I-I″) Higher magnification of the area outlined in H. The boundaries of clones are indicated by broken yellow lines (I′). The most anterior R axon bundles are indicated by arrows (I′). The expression of Hbs (magenta) was markedly decreased in sim^2 clones (n=11). (**J-K″**) Confocal image of the optic lobe immunostained for Hbs in cells overexpressing Sim, which are visualized by GFP (green). pLPCs and LNs are visualized by anti-Dac (blue). (K-K″) Higher magnification of the area outlined in J. The boundaries of cells overexpressing Sim are indicated by broken yellow lines (K′). The most anterior R axon bundles are indicated by arrows (K′). The expression of Hbs (magenta) was increased by forced expression of Sim (n=18).

methods). As a result, we identified *hibris* (*hbs*) as a target of Sim. Hbs is a single-pass transmembrane protein belonging to the immunoglobulin superfamily and has a similarity to the human kidney protein nephrin (Artero et al., 2001; Dworak et al., 2001; Fischbach et al., 2009). To investigate the localization of the Hbs protein in the optic lobe at the late third instar larval stage, we examined its expression by antibody staining. Hbs was localized on the membrane of the pLPCs (Fig. 2A-B″). Note that Hbs seems to accumulate at the contact surface between pLPCs and R axons (Fig. 2B′,D′, arrows, Fig. 2G). Hbs expression in pre-assembling domain was high in the region close to the optic stalk, but lower in cells closer to the lamina plexus (Fig. 2F′, white circle, Fig. 2G). Moreover, Hbs expression in the assembling domain was rather restricted (Fig. 2F′, broken white circle, Fig. 2G). In fact, knockdown of Hbs by RNAi using *NP6099-Gal4*, which specifically expresses Gal4 in pLPCs and LNs (Yoshida et al., 2005), caused downregulation of Hbs in pre-assembling domain and assembling domain (see Fig. S1C-D″ in the supplementary material, 100%: n=8). Hbs was also found to be expressed in R axons (Fig. 2D-D″, arrows) because RNAi knockdown of *hbs* specifically in photoreceptor cells using $ey^{3.5}$*-FLP*; *AyG* (Bazigou et al., 2007) caused downregulation of Hbs in the R axons (see Fig. S1G-G″ in the supplementary material, 100%: n=9), lamina plexus (see Fig. S1H-H″, arrows, in the supplementary material, 100%: n=4) and eye disc (see Fig. S1J′ in the supplementary material, 100%: n=5). Strong staining of Hbs was also observed in the medulla neuropil (Fig. 2E, asterisk) and lobula neuropil (Fig. 2E, double asterisk).

To examine whether *sim* is required for Hbs expression in pLPCs, we analyzed the expression of Hbs in sim^2 mutant clones. Hbs was significantly reduced in sim^2 mutant clones in a cell-autonomous manner (Fig. 2H-I″, 100%: n=11). Consistent with this finding, Hbs was upregulated by forced expression of Sim in pLPCs (Fig. 2J-K″, 100%: n=18). These results indicate that the expression of Hbs is regulated by Sim in pLPCs. In addition, *hbs* expression in the mesectoderm was absent in the *sim* mutant embryo (Dworak et al., 2001).

The extracellular domain of Hbs is essential for the association of pLPCs with R axons

To examine the function of Hbs in pLPCs, we observed the third instar larval brains of *hbs* loss-of-function mutants. pLPCs start to be associated with R axons and assemble into lamina columns

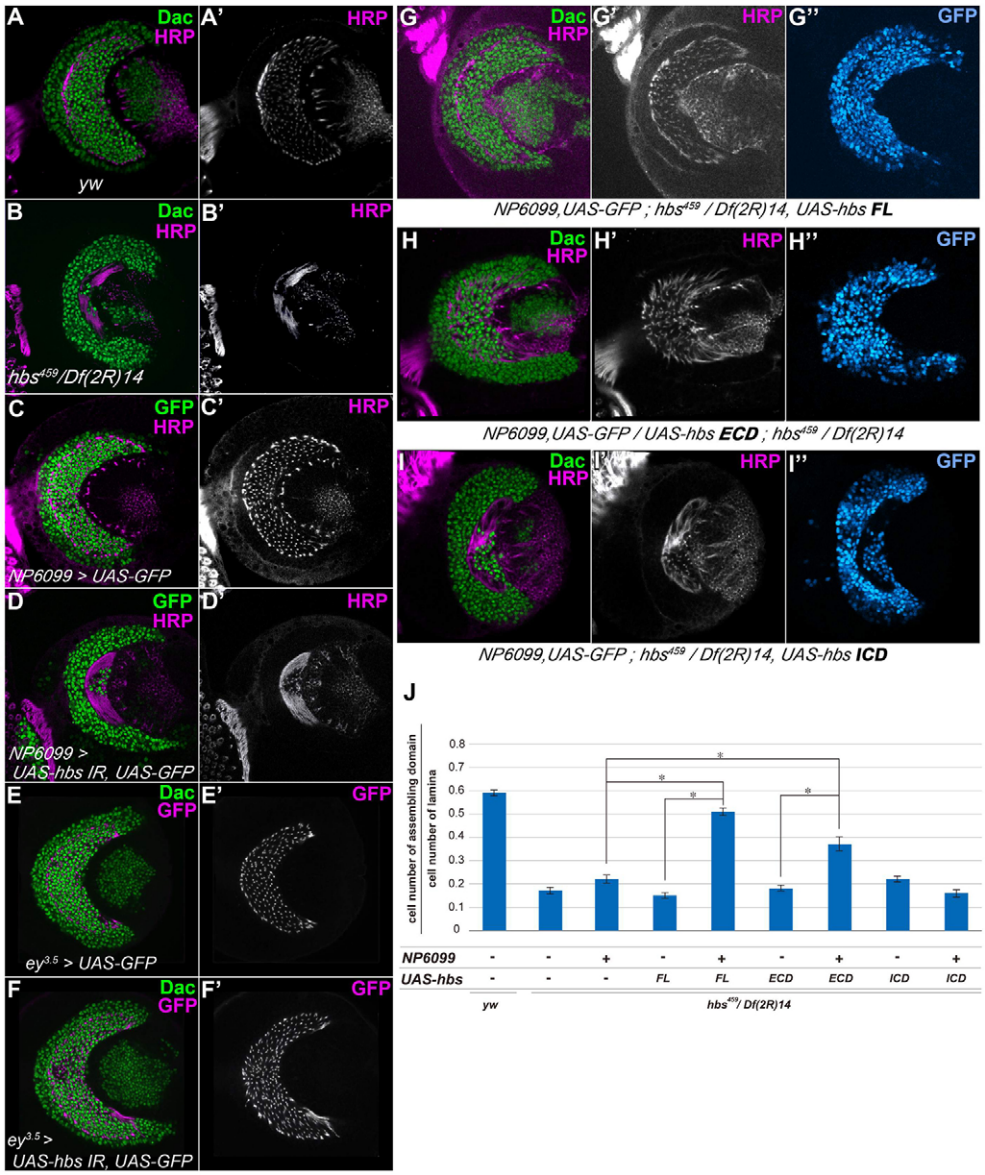

Fig. 3. The expression of Hbs in pLPCs is required and sufficient for the association of pLPCs with R axons. (**A-B′**) The phenotype of the *Drosophila hbs* mutant is shown. pLPCs were incorporated into the assembling domain in *yw* (A, 0.59: *n*=25), but not hbs^{459}*/Df(2R)14* mutants (B, 0.17: *n*=32). (**C-D′**) The phenotype of *hbs* RNAi in pLPCs of *NP6099-Gal4, UAS-GFPnls* (C, 0.63: *n*=5) and *NP6099-Gal4, UAS-GFPnls; UAS-hbs IR; UAS-dicer2* (D, 0.20: *n*=10). Cells expressing *gal4* are marked by the expression of GFP (green). (**E-F′**) The phenotype of *hbs* RNAi in photoreceptor cells of $ey^{3.5}$*-FLP;AyG, UAS-GFP* (E, 0.56: *n*=5) and $ey^{3.5}$*-FLP;AyG, UAS-GFP/UAS-hbs IR* (F, 0.60: *n*=5). R axons are visualized by $ey^{3.5}$*-FLP; AyG, UAS-GFP* (E,F, magenta; E′,F′, white). (**G-I″**) Rescue of the *hbs* mutation by different *hbs* constructs driven by *NP6099-Gal4*. *NP6099-Gal4, UAS-GFPnls;* hbs^{459}*/Df(2R)14, UAS-hbs FL* (G), *NP6099-Gal4, UAS-GFPnls / UAS-hbs ECD;* hbs^{459}*/Df(2R)14* (H) and *NP6099-Gal4, UAS-GFPnls;* hbs^{459}*/ Df(2R)14, UAS-hbs ICD* (I). Cells expressing *hbs* (*FL, ECD* or *ICD*) are marked by the expression of GFP (G″-I″, blue). pLPCs and LNs are visualized by anti-Dac (A,B,E-I, green). R axons are visualized by anti-HRP (A-I, magenta; A′-I′, white). (**J**) Quantification of lamina column defects in animals carrying the construct, as described. The ratio of the number of Dac-positive cells of the assembling domain to that of the lamina was calculated. Expression of exogenous *hbs FL* and *ECD* fragments in pLPCs significantly rescued the *hbs* mutation. *yw* (0.59: *n*=25), hbs^{459}*/Df(2R)14* (0.17: *n*=32), *NP6099-Gal4,UAS-GFPnls;*hbs^{459}*/Df(2R)14* (0.22: *n*=14), hbs^{459}*/Df(2R)14,UAS-hbs FL* (0.15: *n*=23), *NP6099-Gal4,UAS-GFPnls;*hbs^{459}*/Df(2R)14,UAS-hbs FL* (0.51: *n*=15), *UAS-hbs ECD;*hbs^{459}*/Df(2R)14* (0.18: *n*=25), *NP6099-Gal4,UAS-GFPnls/UAS-hbs ECD;*hbs^{459}*/Df(2R)14* (0.37: *n*=27), hbs^{459}*/Df(2R)14,UAS-hbs ICD* (0.22: *n*=15), *NP6099-Gal4,UAS-GFPnls;*hbs^{459}*/Df(2R)14,UAS-hbs ICD* (0.16: *n*=16). These samples were compared and analyzed using Student's *t*-test. Statistical significance (**P*<0.001) is indicated. Error bars represent the standard error of the mean (s.e.m.).

after the developmental stage when ommatidial differentiation has proceeded to 11-12 rows in the eye disc (Umetsu et al., 2006). We therefore examined the phenotype of the lamina column assembly well after this stage of development: at the stage of 16 to 17 rows of ommatidial differentiation or later in the third larval instar (120 hours AEL). As in the *sim* mutant, many pLPCs remained in the pre-assembling domain in the *hbs* mutants (Fig. 3B). The number of Dac-positive cells of the assembling domain within the total Dac-positive lamina cell population was measured to quantify the expressivity of the phenotype. The typical value was 0.59 (*n*=25) for the *yw* control (see Fig. S2A,B,J in the supplementary material) and 0.17

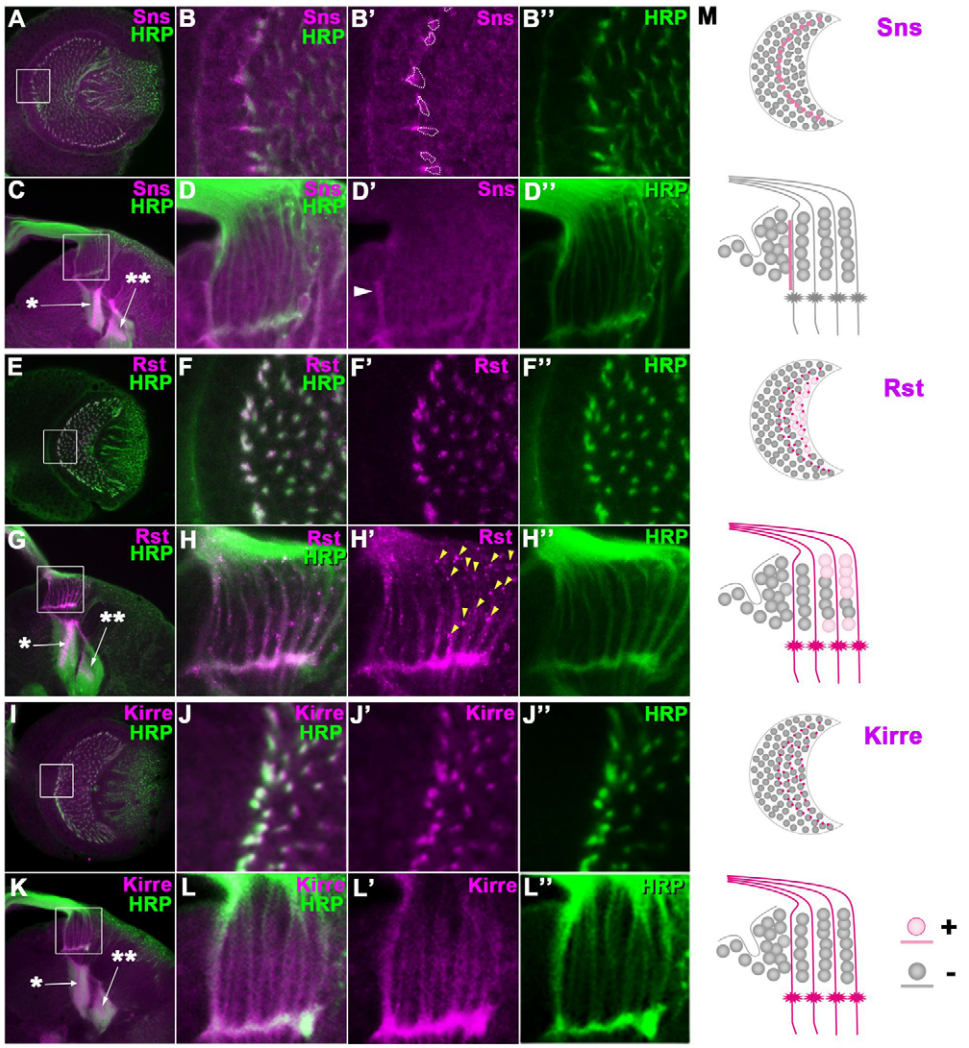

Fig. 4. The expression pattern of *Drosophila* nephrin/NEPH1 homologs. (**A-L″**) Confocal images of the *Drosophila* optic lobe immunostained for Sns (A-D″, magenta), Rst (E-H″, magenta) and Kirre (I-L″, magenta) in *yw*. Sns is localized in the contact surface between pLPCs and R axons (B′, broken white lines; D′, white arrowhead). Rst and Kirre are localized in R axons (F,F′,H,H′,J,J′,L,L′). Rst expression is also observed in the posterior region of the developing lamina (H′, yellow arrowheads). The medulla neuropil (asterisk) and lobula neuropil (double asterisk) are also stained by Sns (C), Rst (G) and Kirre (K). Lateral sections (A,E,I) and horizontal sections (C,G,K) of the optic lobe are shown. (B-B″,D-D″,F-F″,H-H″,J-J″,L-L″) Magnified images of the areas outlined in A,C,E,G,I,K. R axons are visualized by anti-HRP (green). (**M**) Schematic drawings of Sns, Rst and Kirre staining. The stained region (+) is shown in magenta.

(*n*=32) for the *hbs*^{459}*/Df(2R)14* mutants (see Fig. S2C,D,J in the supplementary material). Similar results were obtained at the white pupal stage (see Fig. S2G-H′,J in the supplementary material), suggesting that the phenotype of the *hbs* mutants is not due to a delay in development. Knockdown of Hbs by RNAi using *NP6099-Gal4* also caused an accumulation of pLPCs in the pre-assembling domain that resembled the phenotype observed in the *hbs*^{459}*/Df(2R)14* mutants (Fig. 3D, 0.20: *n*=10), suggesting that Hbs in pLPCs is required for the lamina column assembly. We then asked whether Hbs expression in pLPCs is sufficient for the association of pLPCs with R axons. We expressed exogenous *hbs* in *hbs*^{459}*/Df(2R)14* mutants using *NP6099-Gal4*. We found that lamina column assembly was significantly rescued (Fig. 3G-G″,J, 0.51: *n*=15), providing strong evidence that *hbs* is autonomously required in pLPCs for lamina column assembly. Although Hbs was also expressed in R axons, knockdown of Hbs function in photoreceptor cells did not show defects in lamina column assembly (Fig. 3F, 0.60: *n*=5). Exogenously supplied *hbs* in the photoreceptor cells in the background of the *hbs*^{459}*/Df(2R)14* mutant did not rescue the defects (Fig. 5G-G″,H, 0.16: *n*=20). Hbs overexpressed in the photoreceptor cells caused no morphological defect in the lamina (see Fig. S3C-D″ in the supplementary material, 0.54: *n*=9). These results indicate that *hbs* expressed in the photoreceptor cells does not play an essential role in lamina column assembly.

R axon projections into the medulla layer in *hbs*^{459}*/Df(2R)14* were indistinguishable from those of *yw* (see Fig. S4A-D′ in the supplementary material), indicating that the phenotype was caused by a failure in the interaction between pLPCs and R axons, but not by a global pathfinding defect of R axons.

To identify functional domains of Hbs, we performed a series of rescue experiments with different Hbs fragments encoded in *UAS-hbs ECD* (transmembrane and extracellular domain) and *UAS-hbs ICD* (transmembrane and intracellular domain) (Artero et al., 2001). These constructs were expressed using the *NP6099-Gal4* driver. We found that the expression of the ECD of Hbs could rescue lamina column assembly in *hbs*^{459}*/Df(2R)14*, albeit with lower efficiency than full-length Hbs (Fig. 3H-H″,J, 0.37: *n*=27). The expression of ICD, however, did not rescue the phenotype (Fig. 3I-I″,J, 0.16: *n*=16). These results suggest that the extracellular domain of Hbs is essential for the association of pLPCs with R axons.

nephrin/NEPH1 homologs are expressed in the optic lobe and photoreceptors

We next searched for other nephrin and NEPH1 homologs that play a role in R axons as a partner of Hbs. These homologs are suggested to function through direct interactions between Hbs and IrreC/Roughest (Rst) (Bao and Cagan, 2005), Sticks-and-stones (Sns) and Kin of irre (Kirre, also called Dumbfounded) (Galletta et

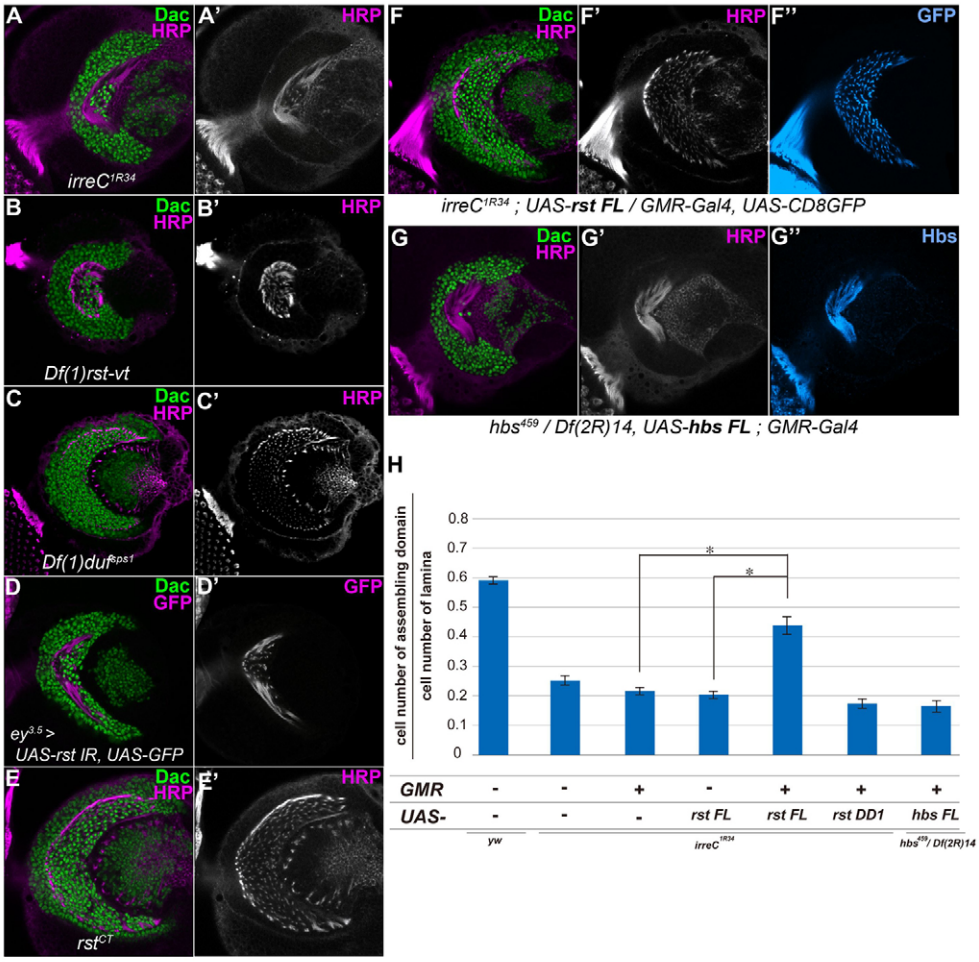

Fig. 5. Rst is required for the incorporation of pLPCs into the assembling domain. (**A-C′**) The phenotype of *Drosophila rst* and *kirre* mutants. pLPCs were incorporated into the assembling domain in *Df(1)dus*^{sps1}(C, 0.60: *n*=11), but not in *irreC*^{1R34} (A, 0.25: *n*=24) or *Df(1)rst-vt* mutants (B, 0.27: *n*=6). (**D,D′**) The phenotype of *rst* RNAi using *ey*$^{3.5}$*-FLP;AyG, UAS-GFP*. Knockdown of Rst function in the R axons resulted in a phenotype similar to, but less severe than, that of the *rst* mutants (0.31: *n*=27). R axons are visualized by *ey*$^{3.5}$*-FLP; AyG, UAS-GFP* (D, magenta; D′, white). (**E,F′**) The phenotype of the *rst* mutant. pLPCs were incorporated into the assembling domain in the *rst*^{CT} mutants (0.61: *n*=3). (**F-G″**) The expression of eye-specific *GMR-Gal4* used for rescue experiments in *rst* or *hbs* mutants. *irreC*^{1R34}*;UAS-rst FL/GMR-Gal4* (F-F″) and *hbs*^{459}*/Df(2R)14;GMR-Gal4* (G-G″). pLPCs and LNs are visualized using anti-Dac (green) and R axons are visualized using anti-HRP (A-C,E-G, magenta; A′-C′,E′-G′, white). (**H**) Quantification of lamina column defects in animals carrying constructs, as described. The ratio of the number of Dac-positive cells of the assembling domain to that of the total pLPCs and LNs was calculated. Expression of exogenous *rst* in photoreceptor cell occasionally rescued lamina column assembly. *yw* (0.59: *n*=25), *irreC*^{1R34} (0.25: *n*=24), *irreC*^{1R34}*;GMR-Gal4,UAS-CD8GFP* (0.21: *n*=34), *irreC*^{1R34}*;UAS-rst FL* (0.20: *n*=22), *irreC*^{1R34}*;UAS-rst FL/GMR-Gal4,UAS-CD8GFP* (0.44: *n*=19), *irreC*^{1R34}*;UAS-rst-DD1/GMR-Gal4,UAS-CD8GFP* (0.17: *n*=13) and *hbs*^{459}*/Df(2R)14,UAS-hbs FL;GMR* (0.16: *n*=20). These samples were compared and analyzed using Student's *t*-test. Statistical significance (*P<0.001) is indicated. Error bars represent the standard error of the mean (s.e.m.).

al., 2004) and Hbs and Sns (Shelton et al., 2009). We therefore examined the localization patterns of the nephrin homolog Sns. We found that Sns was localized in the region in which pLPCs and R axons come into contact with each other (Fig. 4A-D″,M). To elucidate the tissue in which Sns is expressed, we examined the effect of Sns knockdown by RNAi in pLPCs or photoreceptor cells. Knockdown of Sns by RNAi using *NP6099-Gal4* decreased the Sns level in the region in which pLPCs and R axons come into contact with each other (see Fig. S5C-D″ in the supplementary material, 100%: *n*=7). However, RNAi against *sns* using *ey*$^{3.5}$*-FLP*; *AyG* did not cause downregulation of Sns (see Fig. S5G-H″ in the supplementary material, 100%: *n*=7). Moreover, we did not detect Sns expression in the eye disc (see Fig. S5I-J′ in the supplementary material). These results indicate that Sns is expressed in pLPCs. Knockdown of Sns by RNAi in pLPCs did not result in defects in lamina column assembly (see Fig. S5C-D″ in the supplementary material, 0.62: *n*=5), suggesting that Sns expressed in pLPCs is dispensable for this process.

Two NEPH1 homologs Rst and Kirre were apparently localized in R axons (Fig. 4E-M). To confirm this finding, we reduced the expression of these proteins by RNAi in pLPCs or photoreceptor cells. Knockdown of Rst or Kirre by RNAi using *NP6099-Gal4* did not reduce the signal of Rst (see Fig. S6C-D″ in the supplementary material, 100%: *n*=9) or Kirre (see Fig. S6G-H″ in the supplementary material, 100%: *n*=5) in the region in which pLPCs and R axons come into contact with each other. By contrast, RNAi against *rst* and *kirre* using *ey*$^{3.5}$*-FLP*; *AyG* caused a substantial reduction in the expression of Rst (see Fig. S6K-L″ in the supplementary material, 100%: *n*=7) and Kirre (see Fig. S6O-P″ in the supplementary material, 100%: *n*=10), indicating that Rst and

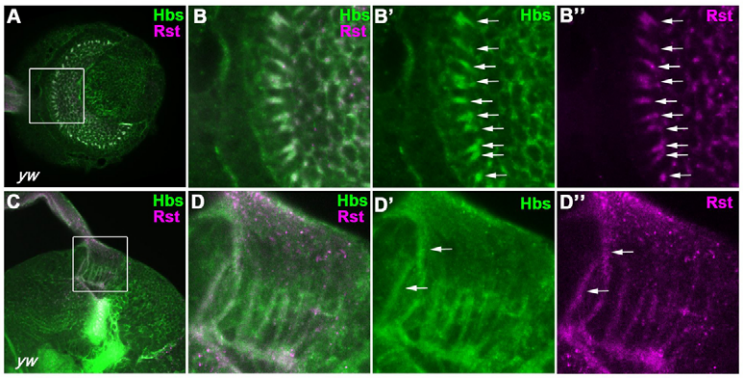

Fig. 6. The expression patterns of Hbs and Rst. (**A-D″**) Confocal images of the *Drosophila* optic lobe immunostained for Hbs (green) and Rst (magenta) in *yw*. Hbs and Rst are localized in R axons and at the contact surface between pLPCs and R axons (arrows). Lateral section (A) and horizontal section (C) of the optic lobe. (B-B″,D-D″) Magnified images of the areas outlined in A and C.

Kirre are expressed in photoreceptor cells. We also detected punctate expression of Rst in the assembling domain (Fig. 4H′, yellow arrowheads). This expression was derived from LNs because knockdown of Rst by RNAi using *NP6099-Gal4* caused a loss of the punctate expression of Rst in the assembling domain (see Fig. S6D-D″ in the supplementary material, 100%: *n*=9), but knockdown of Rst by RNAi using *ey*$^{3.5}$*-FLP*; *AyG* did not (see Fig. S6L-L″ in the supplementary material, yellow arrowheads, 100%: *n*=7). Knockdown of Rst by RNAi in LNs did not result in defects in lamina column assembly (see Fig. S6C-C″ in the supplementary material, 0.61: *n*=3), suggesting that Rst expressed in LNs is dispensable for lamina column assembly. Three nephrin/NEPH1 homologs were also detected in the medulla neuropil (Fig. 4C,G,K, asterisk) and lobula neuropil (Fig. 4C,G,K, double asterisks). The above results suggest that Rst and Kirre are candidate partners of Hbs in R axons.

Rst is a partner of Hbs in R axons

We tested whether the heterophilic interaction between Hbs in pLPCs and Rst and/or Kirre on R axons plays a role in lamina column assembly. In the brain of *irreC*^{1R34}, a null *rst* mutant, R axons were not associated with pLPCs (Fig. 5A, 0.25: *n*=24), as in *hbs*^{459}*/Df(2R)14* mutants. A similar phenotype was observed in *Df(1)rst-vt*, a mutant that is deficient for *kirre* and *rst* (Fig. 5B, 0.27: *n*=6). However, *Df(1)duf*$^{[sps1]}$, which lacks only *kirre* function, did not show this phenotype (Fig. 5C, 0.60: *n*=11). In addition, we confirmed that RNAi specifically targeting *rst* in photoreceptor cells using *ey*$^{3.5}$*-FLP*; *AyG* phenocopied the mutant phenotype (Fig. 5D, 0.31: *n*=27). These results indicate that Rst in R axons is required for lamina column assembly. As in the case of *hbs*, the *rst* phenotype was not due to a delay in the development of the visual system (see Fig. S2E,F,I,J in the supplementary material) or to a global pathfinding defect of R axons (see Fig. S4E in the supplementary material).

To further confirm the role of Rst, we performed a rescue experiment in which a transgene of *rst* was expressed in photoreceptor cells in the mutant background. The ratio of lamina column assembly was measured as described previously. The expression of *rst* in photoreceptor cells rescued the defect in lamina column assembly in *irreC*^{1R34} mutant brains (Fig. 5F-F″,H, 0.44: *n*=19), indicating that *rst* expressed in photoreceptor cells plays an essential role in lamina column assembly.

The mutant allele *rst*^{CT}, which lacks the intracellular domain and thus cannot transduce the signal, but is capable of mediating cell-cell adhesion (Schneider et al., 1995), had no effects on lamina column assembly (Fig. 5E, 0.61: *n*=3). This result suggests that adhesion, rather than intracellular signaling of Rst, plays an important role in lamina column assembly. In addition, the lamina column defect was not rescued with *UAS-rst-DD1*, which lacks the first Ig domain of Rst (Vishnu et al., 2006) (Fig. 5H, 0.17: *n*=13), again confirming the importance of Rst as an adhesion molecule.

Hbs interacts with Rst at the interface between pLPCs and R axons

Hbs in pLPCs was not only localized on the plasma membrane, but presumably also accumulated at the contact surface between pLPCs and R axons (Fig. 6A-B′,C-D′, arrows). Rst was localized in R axons (Fig. 6B″,D″, arrows), suggesting these proteins can associate directly each other. As shown by immunoprecipitation assay, Hbs directly interacts with Rst (Bao and Cagan, 2005). This finding prompted us to ask whether Hbs localization is dependent on Rst in R axons. To confirm Hbs-Rst association, we analyzed the localization of Hbs in *rst* mutants. An RNAi-induced reduction in Rst levels (Fig. 7C-D″, 100%: *n*=13) or the *irreC*^{1R34} mutation (Fig. 7E-F″, 100%: *n*=18) led to consistent and significant changes in Hbs localization; the pronounced Hbs signal at the interface between pLPCs and R axons became less clear, and the membranous signal encircling the entire cell surface became more evident. To confirm the changes in Hbs localization specifically in pLPCs, we used an HA-tagged version of Hbs (Shelton et al., 2009) as Hbs is also expressed in R axons. Hbs-HA was expressed by the *NP6099-Gal4* driver and detected with an anti-HA antibody. The Hbs-HA signal was more punctate than the endogenous Hbs signal, as revealed by antibody staining, but was localized at the interface between pLPCs and R axons as seen for endogenous Hbs (Fig. 7G-I, arrows; *n*=19). The Hbs-HA localization at the interface between pLPCs and R axons became less clear and more evident in the plasma membrane in *rst* mutants (Fig. 7J-L, 100%: *n*=20), similar to endogenous Hbs (Fig. 7E-F″). These results suggest that Hbs in pLPCs directly associates with Rst in R axons.

To further address the interaction between Hbs and Rst, we examined Hbs localization in pLPCs when Rst was ectopically expressed with the *NP6099-Gal4* driver. Ectopic Rst expression in pLPCs resulted in phenotypes that were almost identical to those observed with the *rst* mutation; failure in assembling the lamina column and changes in the localization of endogenous Hbs (see Fig. S7 in the supplementary material, 100%: *n*=14) and Hbs-HA (Fig. 7M-R, 100%: *n*=20) from the contact site to the entire plasma membrane were observed, suggesting that ectopically expressed Rst interferes with the interaction between Hbs in pLPCs and Rst in R axons. Although we cannot rule out the possibility of an existing third molecule, our data strongly suggest that the cell-cell association between pLPCs and R axons is mediated by an interaction between Hbs and Rst.

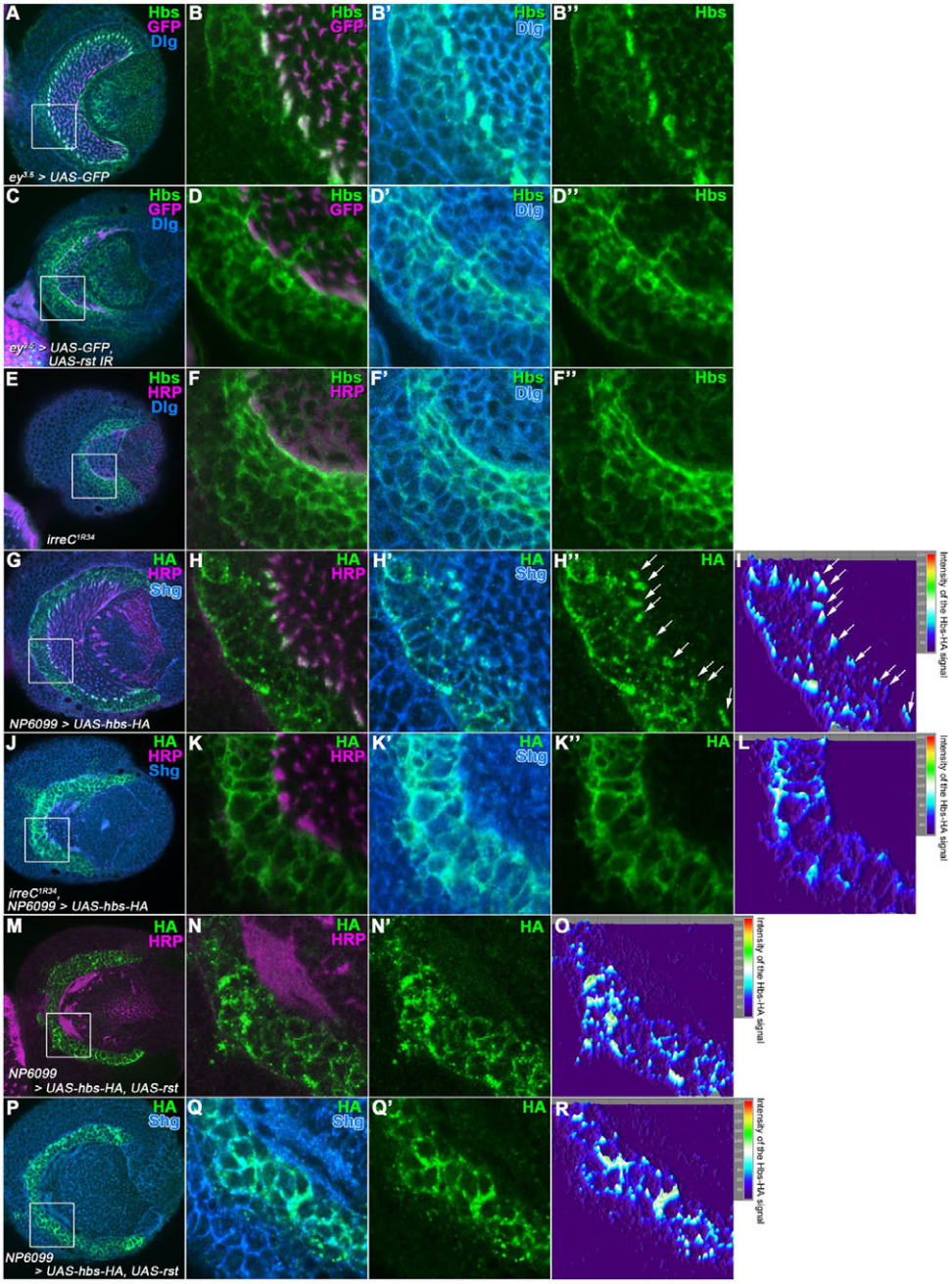

Fig. 7. The localization of Hbs is dependent on Rst. (**A-F″**) The localization patterns of the Hbs protein (green) in the lateral view of the lamina in *ey$^{3.5}$-FLP;AyG,UAS-GFP* (A-B″), *ey$^{3.5}$-FLP;AyG,UAS-GFP/UAS-rst IR* (C-D″) and *irreC^{1R34}* (E-F″). The Hbs membranous signal encircling the entire cell surface became more evident in an RNAi against Rst (C-D″) or the *irreC^{1R34}* mutation (E-F″). (B-B″,D-D″,F-F″) Magnified images of the areas outlined in A,C,E, respectively. R axons are visualized by GFP (A-D, magenta) and anti-HRP (E,F, magenta). Plasma membranes are visualized by anti-Dlg (blue). (**G-R**) The localization patterns of *UAS-hbs-HA* (green) by crossing with the *NP6099-Gal4* driver. *NP6099-Gal4;UAS-hbs-HA* (G-I), *irreC^{1R34},NP6099-Gal4;UAS-hbs-HA* (J-L) and *NP6099-Gal4;UAS-hbs-HA/UAS-rst FL* (M-R). Arrows (H″,I) indicate that Hbs-HA was localized along the most anterior part of the R axons. The Hbs-HA localization becomes evident in the plasma membrane in *rst* mutants (J-L). Ectopic Rst expression in pLPCs results in lamina column defects and changes in the localization of Hbs-HA from the contact site to the entire plasma membrane (M-R). (H-H″,K-K″,N,N′,Q,Q′) Magnified images of the areas outlined in G,J,M,P. R axons are visualized by anti-HRP (magenta). Plasma membranes are visualized by anti-Shg (blue). (I,L,O,R) 2.5D images of Hbs-HA expression. Intensity of the Hbs-HA signals in H″,K″,N′,Q′ is visualized by the height of the peaks.

DISCUSSION

In this study, we show that cell recognition between pre- and postsynaptic neurons via the Hbs-Rst interaction is required for the establishment of precise retinotopic mapping. During the development of the *Drosophila* visual center, presynaptic photoreceptors extend their axons to the lamina layer. Postsynaptic pLPCs start to differentiate in response to Hh delivered through newly arriving R axons. They then express Hbs, which interacts with Rst on R axons. This Hbs-Rst interaction is required for lamina column assembly (Fig. 8), which underlies the topographic connections of the synapses along the anteroposterior axis.

Cell recognition by Hbs-Rst interaction

The process of lamina column assembly is unique in that presynaptic neurons regulate the development of postsynaptic partners in the target area, and the somata of postsynaptic neurons recognize the presynaptic axons at the developing stage well before neurite formation. This mechanism appears to be an efficient and accurate way to make a topographic map along the anterior/posterior axis. In addition, unlike the well-known axon guidance process, in which growth cones search for their targets (Dickson, 2002; Guan and Rao, 2003; Tessier-Lavigne and Goodman, 1996; Yu and Bargmann, 2001), postsynaptic cells actively contribute to the pre- and postsynaptic interactions via direct communication. The changes in the Hbs localization that are associated with *rst* mutation were not only observed in pLPCs adjacent to R axons, but also in pLPCs far from R axons (Fig. 7D-D″,F-F″,K-K″). This finding could be ascribed to the fact that pLPCs that are distant from R axons can contact R axons through their protrusions, as shown in Fig. 1G. Hbs might be preferentially localized at the protrusions of pLPCs that interact with R axons. The behavior of pLPCs is analogous to

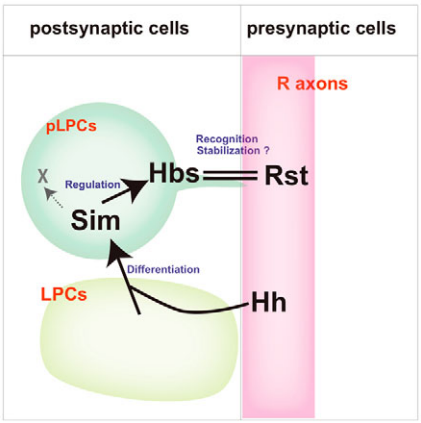

Fig. 8. Model for the specific interaction between R axons and pLPCs mediated by an interaction between Hbs and Rst. Schematic illustration of the first step of lamina column assembly in *Drosophila*. LPCs that receive Hh from R axons start to express Sim and differentiate into pLPCs. Sim then induces Hbs expression, and an Hbs-Rst interaction enables pLPCs to associate with R axon bundles.

that of developing muscle cells, which extend filopodia to the axonal targeting of innervating motoneurons (Kohsaka and Nose, 2009; Ritzenthaler et al., 2000).

We tested whether the cell-adhesion mechanism mediated by Hbs and Rst was sufficient to rescue the *sim* phenotypes. Induction of exogenous *hbs* in pLPCs did not rescue *sim* loss-of-function mutants (data not shown). Consistent with this finding, overexpression of *sim* using the *NP6099-Gal4* driver caused the premature incorporation of pLPCs into the assembling domain (Umetsu et al., 2006), but overexpression of *hbs* did not (see Fig. S3A-B″ in the supplementary material, 0.62: n=3). These results suggest that other molecules under the control of *sim* must be required for lamina column assembly.

We demonstrated that *hbs* expressed in photoreceptor cells does not play an essential role in lamina column assembly (Fig. 3F,G-G″). The reason that Hbs originating in R axons does not interfere with the Hbs-Rst association remains unknown. The intracellular interaction of the two proteins might be blocked in R axons as a result of alternative subcellular localization and/or steric hindrance, or additional intermediates might be required for Hbs function in pLPCs, but not in R axons.

Possible conserved roles of the restricted domains of nephrin/NEPH1 homologs

Nephrin and NEPH1 homolog proteins tend to be located on opposing cell membranes so that they are brought into close apposition. This arrangement underlies the amazingly similar patterns of immunoreactivity in the eye disc, wing disc and somatic muscle as well as in the pupal optic lobe (Bao and Cagan, 2005; Dworak and Sink, 2002; Fischbach et al., 2009). We also found that these proteins are located in opposing cell membranes in the lamina. Consistent with previous studies, Hbs and Sns proteins were expressed in pLPCs (Fig. 2A-B″,G; Fig. 4A-D″,M), whereas Rst and Kirre were expressed in R axons (Fig. 4E-H″,I-L″,M); however, Hbs was also expressed in R axons (Fig. 2C-F″). Recent studies have demonstrated that proteins of the nephrin and NEPH subfamilies are also expressed in neighboring cell types in vertebrate nervous systems (Beltcheva et al., 2003; Gerke et al., 2006; Morikawa et al., 2007; Serizawa et al., 2006; Tamura et al., 2005). These observations reveal the conservation of nephrin/NEPH1 expression patterns across tissues and species.

Previously, Shen and colleagues identified SYG-1, a homolog of Rst, Kirre and NEPH1, as well as SYG-2, a homolog of Hbs, Sns and nephrin, which are necessary for synaptic specificity in *Caenorhabditis elegans* (Shen et al., 2004). These authors found that the first Ig domain of SYG-1 and the first five Ig domains of SYG-2 are necessary and sufficient for binding and synapse formation in vivo (Chao and Shen, 2008). Similarly, we found that the extracellular domain of Hbs and the first Ig domain of Rst are important for the association of pLPCs with R axons (Fig. 3J; Fig. 5H). These observations show remarkable functional conservation of the restricted domains of *Drosophila* and *C. elegans* nephrin/NEPH1 homologs.

Further study of the preferential cell adhesion between nephrin/NEPH1 homolog proteins may reveal a common mechanism underlying the interaction between pre- and postsynaptic neurons in both *Drosophila* and vertebrate brains.

Acknowledgements

We thank T. Shimada and K. Ito for providing a developmental version of the Eve software. We thank members of Tabata laboratory for helpful discussions. We also thank Y. Maeyama for her excellent technical help. We are grateful to S. Abmayr, R. Cagan, W. Chia, T. Clandinin, H. Skaer, the Bloomington Stock Center, the National Institute of Genetics, the Drosophila Genetic Resource Center Kyoto and Vienna Drosophila RNAi Center for fly strains, and DSHB for antibodies. This work was supported by MEXT, Global COE Program (Integrative Life Science Based on the Study of Biosignaling Mechanisms), the Toray Science and Technology Grant, and Yamada Science foundation. A Predoctoral Fellowship provided support for A.S. from JSPS.

Competing interests statement

The authors declare no competing financial interests.

Supplementary material

Supplementary material for this article is available at
http://dev.biologists.org/lookup/suppl/doi:10.1242/dev.047332/-/DC1

References

Artero, R. D., Castanon, I. and Baylies, M. K. (2001). The immunoglobulin-like protein Hibris functions as a dose-dependent regulator of myoblast fusion and is differentially controlled by Ras and Notch signaling. *Development* **128**, 4251-4264.

Bao, S. and Cagan, R. (2005). Preferential adhesion mediated by Hibris and Roughest regulates morphogenesis and patterning in the *Drosophila* eye. *Dev. Cell* **8**, 925-935.

Barclay, J. W. and Robertson, R. M. (2003). Role for calcium in heat shock-mediated synaptic thermoprotection in *Drosophila* larvae. *J. Neurobiol.* **56**, 360-371.

Bazigou, E., Apitz, H., Johansson, J., Loren, C. E., Hirst, E. M., Chen, P. L., Palmer, R. H. and Salecker, I. (2007). Anterograde Jelly belly and Alk receptor tyrosine kinase signaling mediates retinal axon targeting in *Drosophila*. *Cell* **128**, 961-975.

Beltcheva, O., Kontusaari, S., Fetissov, S., Putaala, H., Kilpelainen, P., Hokfelt, T. and Tryggvason, K. (2003). Alternatively used promoters and distinct elements direct tissue-specific expression of nephrin. *J. Am. Soc. Nephrol.* **14**, 352-358.

Bour, B. A., Chakravarti, M., West, J. M. and Abmayr, S. M. (2000). *Drosophila* SNS, a member of the immunoglobulin superfamily that is essential for myoblast fusion. *Genes Dev.* **14**, 1498-1511.

Chang, J., Jeon, S. H. and Kim, S. H. (2003). The hierarchical relationship among the spitz/Egfr signaling genes in cell fate determination in the *Drosophila* ventral neuroectoderm. *Mol. Cells* **15**, 186-193.

Chao, D. L. and Shen, K. (2008). Functional dissection of SYG-1 and SYG-2, cell adhesion molecules required for selective synaptogenesis in *C. elegans*. *Mol. Cell. Neurosci.* **39**, 248-257.

Clandinin, T. R. and Zipursky, S. L. (2002). Making connections in the fly visual system. *Neuron* **35**, 827-841.

Denholm, B., Sudarsan, V., Pasalodos-Sanchez, S., Artero, R., Lawrence, P., Maddrell, S., Baylies, M. and Skaer, H. (2003). Dual origin of the renal tubules in *Drosophila*: mesodermal cells integrate and polarize to establish secretory function. *Curr. Biol.* **13**, 1052-1057.

Dickson, B. J. (2002). Molecular mechanisms of axon guidance. *Science* **298**, 1959-1964.
Dworak, H. A. and Sink, H. (2002). Myoblast fusion in *Drosophila*. *BioEssays* **24**, 591-601.
Dworak, H. A., Charles, M. A., Pellerano, L. B. and Sink, H. (2001). Characterization of *Drosophila* hibris, a gene related to human nephrin. *Development* **128**, 4265-4276.
Ferrus, A. (1975). Parameters of mitotic recombination in minute mutants of *Drosophila melanogaster*. *Genetics* **79**, 589-599.
Fischbach, K. F., Linneweber, G. A., Andlauer, T. F., Hertenstein, A., Bonengel, B. and Chaudhary, K. (2009). The irre cell recognition module (IRM) proteins. *J. Neurogenet.* **23**, 48-67.
Galletta, B. J., Chakravarti, M., Banerjee, R. and Abmayr, S. M. (2004). SNS: Adhesive properties, localization requirements and ectodomain dependence in S2 cells and embryonic myoblasts. *Mech. Dev.* **121**, 1455-1468.
Gerke, P., Benzing, T., Hohne, M., Kispert, A., Frotscher, M., Walz, G. and Kretz, O. (2006). Neuronal expression and interaction with the synaptic protein CASK suggest a role for Neph1 and Neph2 in synaptogenesis. *J. Comp. Neurol.* **498**, 466-475.
Guan, K. L. and Rao, Y. (2003). Signalling mechanisms mediating neuronal responses to guidance cues. *Nat. Rev. Neurosci.* **4**, 941-956.
Hay, B. A., Maile, R. and Rubin, G. M. (1997). P element insertion-dependent gene activation in the *Drosophila* eye. *Proc. Natl. Acad. Sci. USA* **94**, 5195-5200.
Hayashi, S., Ito, K., Sado, Y., Taniguchi, M., Akimoto, A., Takeuchi, H., Aigaki, T., Matsuzaki, F., Nakagoshi, H., Tanimura, T. et al. (2002). GETDB, a database compiling expression patterns and molecular locations of a collection of Gal4 enhancer traps. *Genesis* **34**, 58-61.
Huang, Z. and Kunes, S. (1996). Hedgehog, transmitted along retinal axons, triggers neurogenesis in the developing visual centers of the *Drosophila* brain. *Cell* **86**, 411-422.
Huang, Z. and Kunes, S. (1998). Signals transmitted along retinal axons in *Drosophila*: Hedgehog signal reception and the cell circuitry of lamina cartridge assembly. *Development* **125**, 3753-3764.
Huang, Z., Shilo, B. Z. and Kunes, S. (1998). A retinal axon fascicle uses spitz, an EGF receptor ligand, to construct a synaptic cartridge in the brain of *Drosophila*. *Cell* **95**, 693-703.
Hynes, R. O. and Lander, A. D. (1992). Contact and adhesive specificities in the associations, migrations, and targeting of cells and axons. *Cell* **68**, 303-322.
Ito, K., Awano, W., Suzuki, K., Hiromi, Y. and Yamamoto, D. (1997). The *Drosophila* mushroom body is a quadruple structure of clonal units each of which contains a virtually identical set of neurones and glial cells. *Development* **124**, 761-771.
Kamikouchi, A., Shimada, T. and Ito, K. (2006). Comprehensive classification of the auditory sensory projections in the brain of the fruit fly *Drosophila melanogaster*. *J. Comp. Neurol.* **499**, 317-356.
Kesper, D. A., Stute, C., Buttgereit, D., Kreiskother, N., Vishnu, S., Fischbach, K. F. and Renkawitz-Pohl, R. (2007). Myoblast fusion in *Drosophila melanogaster* is mediated through a fusion-restricted myogenic-adhesive structure (FuRMAS). *Dev. Dyn.* **236**, 404-415.
Kohsaka, H. and Nose, A. (2009). Target recognition at the tips of postsynaptic filopodia: accumulation and function of Capricious. *Development* **136**, 1127-1135.
Kreiskother, N., Reichert, N., Buttgereit, D., Hertenstein, A., Fischbach, K. F. and Renkawitz-Pohl, R. (2006). *Drosophila* rolling pebbles colocalises and putatively interacts with alpha-Actinin and the Sls isoform Zormin in the Z-discs of the sarcomere and with Dumbfounded/Kirre, alpha-Actinin and Zormin in the terminal Z-discs. *J. Muscle Res. Cell Motil.* **27**, 93-106.
Lee, T. and Luo, L. (1999). Mosaic analysis with a repressible cell marker for studies of gene function in neuronal morphogenesis. *Neuron* **22**, 451-461.
Meinertzhagen, I. A. and Hanson, T. E. (1993). The development of the opticlobe. In *The Development of Drosophila melanogaster* (ed. M. Bate and A. Martinez Arias), pp. 1363-1491. Cold Spring Harbor: Cold Spring Harbor Laboratory Press.
Morikawa, Y., Komori, T., Hisaoka, T., Ueno, H., Kitamura, T. and Senba, E. (2007). Expression of mKirre in the developing sensory pathways: its close apposition to nephrin-expressing cells. *Neuroscience* **150**, 880-886.
Pielage, J., Steffes, G., Lau, D. C., Parente, B. A., Crews, S. T., Strauss, R. and Klambt, C. (2002). Novel behavioral and developmental defects associated with *Drosophila* single-minded. *Dev. Biol.* **249**, 283-299.
Ramos, R. G., Igloi, G. L., Lichte, B., Baumann, U., Maier, D., Schneider, T., Brandstatter, J. H., Frohlich, A. and Fischbach, K. F. (1993). The irregular chiasm C-roughest locus of *Drosophila*, which affects axonal projections and programmed cell death, encodes a novel immunoglobulin-like protein. *Genes Dev.* **7**, 2533-2547.
Ritzenthaler, S., Suzuki, E. and Chiba, A. (2000). Postsynaptic filopodia in muscle cells interact with innervating motoneuron axons. *Nat. Neurosci.* **3**, 1012-1017.
Ruiz-Gomez, M., Coutts, N., Price, A., Taylor, M. V. and Bate, M. (2000). *Drosophila* dumbfounded: a myoblast attractant essential for fusion. *Cell* **102**, 189-198.
Schneider, T., Reiter, C., Eule, E., Bader, B., Lichte, B., Nie, Z., Schimansky, T., Ramos, R. G. and Fischbach, K. F. (1995). Restricted expression of the irreC-rst protein is required for normal axonal projections of columnar visual neurons. *Neuron* **15**, 259-271.
Serizawa, S., Miyamichi, K., Takeuchi, H., Yamagishi, Y., Suzuki, M. and Sakano, H. (2006). A neuronal identity code for the odorant receptor-specific and activity-dependent axon sorting. *Cell* **127**, 1057-1069.
Shelton, C., Kocherlakota, K. S., Zhuang, S. and Abmayr, S. M. (2009). The immunoglobulin superfamily member Hbs functions redundantly with Sns in interactions between founder and fusion-competent myoblasts. *Development* **136**, 1159-1168.
Shen, K., Fetter, R. D. and Bargmann, C. I. (2004). Synaptic specificity is generated by the synaptic guidepost protein SYG-2 and its receptor, SYG-1. *Cell* **116**, 869-881.
Strunkelnberg, M., Bonengel, B., Moda, L. M., Hertenstein, A., de Couet, H. G., Ramos, R. G. and Fischbach, K. F. (2001). rst and its paralogue kirre act redundantly during embryonic muscle development in *Drosophila*. *Development* **128**, 4229-4239.
Takei, Y., Ozawa, Y., Sato, M., Watanabe, A. and Tabata, T. (2004). Three *Drosophila* EXT genes shape morphogen gradients through synthesis of heparan sulfate proteoglycans. *Development* **131**, 73-82.
Tamura, S., Morikawa, Y., Hisaoka, T., Ueno, H., Kitamura, T. and Senba, E. (2005). Expression of mKirre, a mammalian homolog of *Drosophila* kirre, in the developing and adult mouse brain. *Neuroscience* **133**, 615-624.
Tessier-Lavigne, M. and Goodman, C. S. (1996). The molecular biology of axon guidance. *Science* **274**, 1123-1133.
Ting, C. Y. and Lee, C. H. (2007). Visual circuit development in *Drosophila*. *Curr. Opin. Neurobiol.* **17**, 65-72.
Udin, S. B. and Fawcett, J. W. (1988). Formation of topographic maps. *Annu. Rev. Neurosci.* **11**, 289-327.
Umetsu, D., Murakami, S., Sato, M. and Tabata, T. (2006). The highly ordered assembly of retinal axons and their synaptic partners is regulated by Hedgehog/Single-minded in the *Drosophila* visual system. *Development* **133**, 791-800.
Vishnu, S., Hertenstein, A., Betschinger, J., Knoblich, J.A., Gert de Couet, H. and Fischbach, K. F. (2006). The adaptor protein X11Lalpha/Dmint1 interacts with the PDZ-binding domain of the cell recognition protein Rst in *Drosophila*. *Dev. Biol.* **289**, 296-307.
Weavers, H., Prieto-Sanchez, S., Grawe, F., Garcia-Lopez, A., Artero, R., Wilsch-Brauninger, M., Ruiz-Gomez, M., Skaer, H. and Denholm, B. (2009). The insect nephrocyte is a podocyte-like cell with a filtration slit diaphragm. *Nature* **457**, 322-326.
Yoshida, S., Soustelle, L., Giangrande, A., Umetsu, D., Murakami, S., Yasugi, T., Awasaki, T., Ito, K., Sato, M. and Tabata, T. (2005). DPP signaling controls development of the lamina glia required for retinal axon targeting in the visual system of *Drosophila*. *Development* **132**, 4587-4598.
Yu, T. W. and Bargmann, C. I. (2001). Dynamic regulation of axon guidance. *Nat. Neurosci.* **Suppl. 4**, 1169-1176.
Zhuang, S., Shao, H., Guo, F., Trimble, R., Pearce, E. and Abmayr, S.M .(2009). Sns and Kirre, the *Drosophila* orthologs of Nephrin and Neph1, direct adhesion, fusion and formation of a slit diaphragm-like structure in insect nephrocytes. *Development* **136**, 2335-2344.